The Journal of Experimental Biology 201, 3057–3065 (1998)
Printed in Great Britain © The Company of Biologists Limited 1998
JEB1739

IN VIVO STRAINS IN PIGEON FLIGHT FEATHER SHAFTS: IMPLICATIONS FOR STRUCTURAL DESIGN

WILLIAM R. CORNING AND ANDREW A. BIEWENER*

Department of Organismal Biology and Anatomy, The University of Chicago, 1027 East 57th Street, Chicago, IL 60637, USA

*Author for correspondence and present address: Concord Field Station, Museum of Comparative Zoology, Department of Organismic and Evolutionary Biology, Harvard University, Old Causeway Road, Bedford, MA 01730, USA (e-mail: abiewener@oeb.harvard.edu)

Accepted 27 August; published on WWW 26 October 1998

Summary

To evaluate the safety factor for flight feather shafts, *in vivo* strains were recorded during free flight from the dorsal surface of a variety of flight feathers of captive pigeons (*Columba livia*) using metal foil strain gauges. Strains recorded while the birds flew at a slow speed (approximately 5–6 m s^{-1}) were used to calculate functional stresses on the basis of published values for the elastic modulus of feather keratin. These stresses were then compared with measurements of the failure stress obtained from four-point bending tests of whole sections of the rachis at a similar location. Recorded strains followed an oscillatory pattern, changing from tensile strain during the upstroke to compressive strain during the downstroke. Peak compressive strains were 2.2±0.9 times (mean ± S.D.) greater than peak tensile strains. Tensile strain peaks were generally not as large in more proximal flight feathers. Maximal compressive strains averaged −0.0033±0.0012 and occurred late in the downstroke. Bending tests demonstrated that feather shafts are most likely to fail through local buckling of their compact keratin cortex. A comparison of the mean (8.3 MPa) and maximum (15.7 MPa) peak stresses calculated from the *in vivo* strain recordings with the mean failure stress measured in four-point bending (137 MPa) yields a safety factor of between 9 and 17. Under more strenuous flight conditions, feather stresses are estimated to be 1.4-fold higher, reducing their safety factor to the range 6–12. These values seem high, considering that the safety factor of the humerus of pigeons has been estimated to be between 1.9 and 3.5. Several hypotheses explaining this difference in safety factor are considered, but the most reasonable explanation appears to be that flexural stiffness is more critical than strength to feather shaft performance.

Key words: feather, keratin, pigeon, *Columbia livia*, safety factor, strain, flight, stress.

Introduction

Feathers are among the most prominent of a suite of adaptations that facilitate flight in birds. However, despite considerable attention directed to the aerodynamic, muscular and skeletal requirements of avian flight, the mechanical design constraints imposed by flight forces on flight feather shafts remain largely unexplored. This study presents measurements of the *in vivo* loading regime of feathers during flight and compares these results with the failure stress of feather shafts determined by four-point bending tests in order to determine their safety factor during flight.

Numerous adaptations make birds stiff and strong, but lightweight ‘flying machines’ (Gill, 1995), and the flight feather shafts are no exception. The general design of a feather shaft (or rachis) resembles that of a composite foam sandwich (Hertel, 1966), a structural design used by engineers to maximize strength while minimizing weight (Gibson and Ashby, 1988). The feather shaft largely consists of a hollow, compact keratin cortex enclosing a medullary foam (for a detailed description, see Rutschke, 1976). In a comparison of the material properties of the cortex from the flight feathers of a variety of bird species, Bonser and Purslow (1995) found the Young’s modulus of the cortex to be highly conserved among species and fairly uniform along much of the length of the rachis. In a related study, the compact keratin was found to be approximately 100 times stiffer than the medullary foam (Bonser, 1996), consistent with an earlier finding of Purslow and Vincent (1978) that the medullary foam and transverse septae contribute only 16 % to the overall bending stiffness of the feather shaft. Because the foam appears to play a minor structural role and material properties remain fairly constant along the length of the rachis, it seems likely that most of the differences in strength between parts of individual feather shafts and among species can be attributed to differences in the cross-sectional geometry of the cortex (Bonser, 1996).

Although the *in vitro* bending properties of feathers are fairly well known, little work has been done to examine their loading conditions *in vivo* during flight. Using a quasi-steady aerodynamic model to approximate the forces on bird and bat wing bones during flight, Kirkpatrick (1994) estimated a safety

factor for bird wing bones. However, in order to estimate forces on individual feathers, a more complicated model would be needed to predict accurately the lift distribution of the wing in both the span-wise and chord-wise directions. No such model currently exists. In an attempt to resolve these problems and modeling limitations, we adopt an experimental approach that involves directly bonding strain gauges to the feather rachis to record strains continuously during flight.

Peak strains recorded during these flights are used to calculate a safety factor, defined here as the ratio of failure stress to maximum functional stress. Following Alexander's (1981) theoretical analysis of several determinants of safety factors, this index of relative strength has been calculated for many structures including vertebrate long bones (Biewener, 1993), crab legs (Hahn and LaBarbera, 1993), mollusc shells (Lowell, 1985) and plant stems (Niklas, 1989). However, feather shafts differ fundamentally from these other structures in ways that would suggest that their safety factor may be very low. The 'cost of use' of feathers can be expected to be high in comparison with that of the wing bones because the moment arm of the primary flight feathers about the shoulder joint (the primary axis of wing rotation) is longer, increasing their contribution to the inertial work, or energy, required to flap the wing. It seems probable that the cost of use is the strongest selection agent against birds having heavier, thick-walled flight feather shafts. Correspondingly, the cost of failure of a single feather, in terms of survival or fitness, should be much less than that of a limb bone or plant stem. Reduction in this cost may be mitigated, however, by the fact that broken feathers cannot be repaired and are generally replaced only annually in the wing molt. Since a high cost of use and a low cost of failure are generally associated with low safety factors (Alexander, 1981), we predict that the safety factor of flight feather shafts is similar to or lower than the safety factor of the humerus, which has been estimated to be 1.9–3.5 for strenuous conditions of flight (Biewener and Dial, 1995; Kirkpatrick, 1994).

Materials and methods

Animals, training and a description of the flight course

Four adult Silver King pigeons (*Columba livia*) (body mass 551–668 g) were obtained from a commercial vendor, housed in individual cages (46 cm×36 cm×40 cm) and provided with water, chicken feed and bird seed *ad libitum*. The birds were trained to fly indoors along a 9 m path straight to a perch (1.2 m high) when released by hand. The training period lasted for 1 h per day for a period of 1–2 months.

Strain gauge attachment and data collection

Following training, the birds were mildly anaesthetized (intramuscular injection of 15 mg kg^{-1} ketamine and 1 mg kg^{-1} xylazine), and single-element metal foil strain gauges (FLK 1-11, Tokyo Sokki Kenkyujo, Japan) were attached using self-catalyzing cyanoacrylate adhesive to the dorsal surface of one or, in most cases, two flight feather shafts. Strain gauges were attached approximately 2 cm distal to the calamus (base) of the rachis. The lead wires were then passed underneath the covert feathers, anchored near the elbow joint with 3-0 gauge silk suture tied through the skin, and soldered to a miniature connector (Microtech, Inc.) that was sutured to the skin overlying the thoracic vertebrae.

Flight recordings were made immediately after the birds had recovered fully from the anesthetic (typically 4–6 h later) to prevent the birds from damaging the electronics through excessive preening. The strain signals were transmitted *via* a lightweight shielded cable (approximately 30 g suspended weight) to a conditioning bridge amplifier (Vishay model 2020, Micromeasurements Inc.), sampled at 500 Hz by an analog/digital converter, and stored on a microcomputer for subsequent analysis. High-speed video images (250 frames s^{-1}, Kodak Ektapro, model 1012) and feather shaft strains were recorded simultaneously for some of the flights in order to integrate wing kinematics with the strain recordings. The video images were synchronized with the strain recordings using a custom-built device which sent a voltage pulse to both the A/D converter and a light-emitting diode placed in the field of view of the camera. Successful recordings were obtained from six flight feathers (five primaries and one secondary).

Analysis of feather shaft cross-sectional geometry and failure mode

Following completion of the *in vivo* feather strain recordings, the instrumented feathers were removed from the animals' wings, embedded in fiberglass epoxy resin and sectioned transversely using a band saw. The sectioned ends of the rachis were then polished to smoothness with emery paper. The compact keratin cortex of each cross section was traced using a *camera lucida* (magnified 40× on a Wild M8 dissecting microscope), and the tracings were digitized using a computer graphics tablet (Summasketch Plus).

The digitized sections were then used to calculate the shape parameters considered to be important to the calculation of safety factor in feathers: the second moment of area (I) and the mean wall thickness to radius ratio (t/R) were determined using the following formulae:

$$I = \sum y^2 \mathrm{d}A \qquad (1)$$

and

$$t/R = \frac{2\left(\sqrt{A_{\mathrm{out}}} - \sqrt{A_{\mathrm{in}}}\right)}{2\left(\sqrt{A_{\mathrm{out}}} + \sqrt{A_{\mathrm{in}}}\right)}, \qquad (2)$$

where y is the distance from the neutral axis to an area element ($\mathrm{d}A$) and A_{in} and A_{out} are the areas enclosed by the inner and outer surfaces of the compact keratin cortex.

Three different models were applied to estimate the critical bending moment (M) required to cause failure in the feather shaft: (1) rupture of the tensile surface, in which the shaft was modeled as a beam in bending; (2) local buckling of the compressive surface, in which the rachis was modeled as a thin-walled cylinder with a circular cross section loaded in pure bending (Young, 1989); and (3) 'wrinkling' of the compressive surface, in which the rachis was modeled as a foam sandwich

structure (Gibson and Ashby, 1988). The critical bending moment to cause tensile failure was calculated using the following standard formula from beam theory:

$$M = \frac{I}{\sigma_t c} , \quad (3)$$

where σ_t is the failure stress for feather keratin loaded in tension (226 MPa; Crenshaw, 1980) and c is the maximum value of y. The critical buckling moment to cause local buckling failure of a thin-walled cylinder was calculated as (Young, 1989):

$$M = \frac{KErt^2}{1-\nu^2} , \quad (4)$$

where the constant $K \approx 1$, E is the Young's modulus of feather keratin (2.5 GPa; Bonser and Purslow, 1995; Crenshaw, 1980), r is the mean radius of the cross section, t is the mean wall thickness and ν is Poisson's ratio [a value of 0.35 was used, based on the results obtained for dry wool fibers by Fraser and Macrae (1980); we are unaware of a published value for the Poisson's ratio of feather keratin]. When the rachis is modeled as a foam sandwich, the material properties of both the medullary foam and compact keratin cortex need to be considered, and failure is considered to occur when the keratin cortex wrinkles (Gibson and Ashby, 1988). Wrinkling of the cortex is likely to occur when:

$$M = 2.28wth \sqrt[3]{E_m E_c^2 \left(\frac{\rho_m}{\rho_c}\right)^4} , \quad (5)$$

where w is the width of the sandwich, t is the mean thickness of the top and bottom layers of the cortex, h is the height of the section, E_m and E_c are the Young's moduli of the medulla and cortex, respectively, and ρ_m and ρ_c are the densities of the medulla and cortex, respectively.

Effect of strain gauge reinforcement

Because the rachis is a thin-walled structure, the strain gauges probably provided significant reinforcement to the dorsal surface of the feather shafts to which they were attached during flight. The magnitude of this stiffening effect was estimated using digitized cross sections of feather shafts with the strain gauges attached. Assuming a value of 2.5 GPa for the Young's modulus of feather keratin (Bonser and Purslow, 1995; Crenshaw, 1980) and 5.6 GPa for the strain gauge backing (manufacturer's specifications), values of EI/c of the rachis were calculated with and without the strain gauge present for each recording site. These calculations indicated that gauge reinforcement of the six feather shafts varied from 20 to 62 %, averaging 44±15 % (mean ± S.D., N=6). Strains recorded from each feather shaft were subsequently corrected by the estimate of gauge reinforcement. Subsequent mechanical tests with known applied bending moments showed that these estimates of reinforcement are likely to have been conservative, probably as a result of the high stiffness of the cyanoacrylate adhesive, for which we were unable to obtain a reliable value of Young's modulus from the manufacturer (and which changes over time because of curing and ambient conditions). Errors in I, t/R and c associated with tracing and digitizing the cross sections were found to be less than 5 % on the basis of five repeated measurements of a single cross section.

Tests of mechanical failure

Primary flight feathers collected from killed and molting birds were used in bending tests to determine the failure stress of the compact keratin cortex of the feather rachis. In contrast to earlier mechanical studies (Crenshaw, 1980; Worcester, 1996), the feathers were loaded in four-point bending. This method of loading was chosen in preference to cantilever bending because the non-uniformity of cross-sectional shape and longitudinal curvature of the feather rachis complicate the calculation of local stresses. Three-point bending was avoided because it underestimates the failure stress by neglecting the local crushing stress on the compressive surface at the point of load application and failure. To conduct four-point bending tests, whole section specimens of the rachis, approximately 50 mm in length, were cut from the base of each feather. The ends of the section were rigidly fixed with epoxy resin inside two square brass tubes (cross section 4.8 mm×4.8 mm), leaving approximately 10 mm of the rachis section freely exposed between the brass tubes (see Fig. 1A). The specimens were then loaded to failure in a custom-built four-point bending jig, using a 45 N load cell (A. L. Designs, Inc.). Following the mechanical tests to failure, the free ends of each rachis specimen were embedded in epoxy resin, sectioned and smoothed, as above, to measure I, c and t/R as close as possible to the site of failure. The local stress required to cause failure of the test specimens was calculated from the applied bending moment and cross-sectional geometry using a rearrangement of equation 3:

$$\sigma = \frac{Mc}{I} . \quad (6)$$

In nearly all cases (see Results below), four-point bending was found to involve buckling failure. Because the cross section also flattens as a result of Brazier buckling (Brazier, 1927), the second moment of area (I) tends to decrease as load is applied, causing equation 6 to overestimate the stress at failure. Measurements made from video images recorded during a buckling test (at 30× magnification) indicated only a 6 % decrease in the diameter of the shaft prior to buckling failure. Consequently, equation 6 probably gives a reliable measure of failure stress within the wall of the cortex.

Scanning electron microscopy

Scanning electron micrographs were made from mechanical test specimens loaded to failure in buckling and in tension to provide a detailed view of the fracture surface and additional insight into the mode of failure. The section of the shaft loaded in tension was prepared by cutting a 30 mm×1.5 mm×0.25 mm test piece from the cortex, whereas a whole test section was

used for imaging the surface subjected to buckling failure. The specimens were sputter-coated with a gold film before being imaged with an electron microscope (Amray, model 1810).

Results

In vivo *strain recordings*

The birds flew the 9 m course in approximately 1.8 s, or at a mean flight speed of 5 m s^{-1}. Characteristic of slow flight, the birds typically flew with their body oriented at a steep angle (approximately 30 ° to the horizontal), with wing kinematics that exhibited a prominent wing tip reversal 'figure-of-eight' pattern. *In vivo* strains (Fig. 2A) generally followed the pattern expected for a cantilever beam oscillating in the dorsoventral plane (Fig. 1B). Tensile (+) strains indicate a ventrally oriented force (with respect to the feather, not the body) and compressive (–) strains denote a dorsally directed force. Representative strain recorded from the dorsal surface of a ninth primary feather is shown in Fig. 2A. Regular patterns of strain were generally recorded in all feather shafts, with the tensile and compressive peaks always corresponding to the upstrokes and downstrokes, respectively. The magnitude of peak tensile strain averaged 46±19 % (mean ± S.D., *N*=90) of the magnitude of peak compressive strain for the entire set of recordings. However, the relative magnitude of the peak tensile strain during the upstroke was generally smaller in more proximal feathers (e.g. peak tensile strain averaged 27±14 %, *N*=15, of peak compressive strain in the fourth primary of bird 1 and the second secondary of bird 6 compared with 55±18 %, *N*=15, in the ninth primary of bird 1 and the eighth primary of bird 3; $P<0.01$, unpaired *t*-test; d.f.=28).

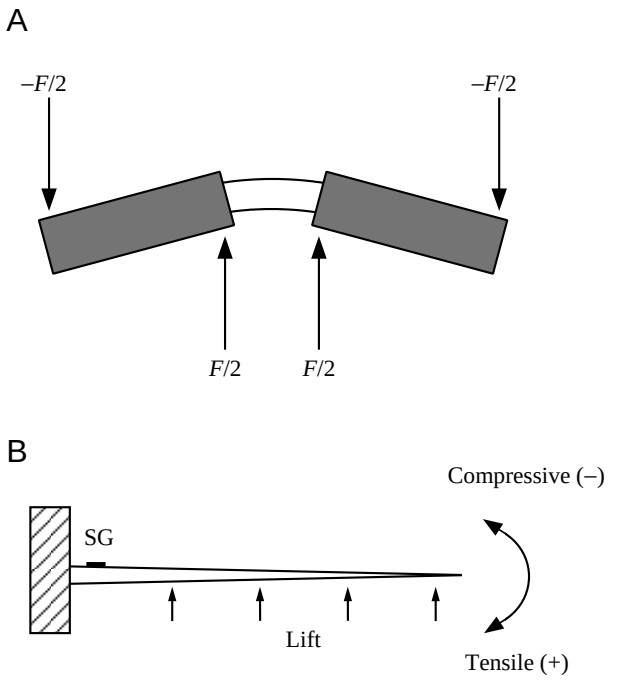

Fig. 1. (A) A schematic diagram of the four-point bending system used in the mechanical tests to failure. Transverse forces (*F*) were applied to 4.8 mm square (in cross section) brass tubes (represented by the shaded rectangles) to avoid exerting local crushing stresses on the feather shaft itself. (B) A schematic diagram of the rachis as it is loaded in flight. The rachis is fixed in place by the base of the wing at the left, with aerodynamic forces acting vertically along its length. Lift forces exert a counterclockwise bending moment about the base, which produces negative, or compressive, strains on the dorsal surface at the site of the strain gauge (SG). Note that this loading scheme oversimplifies the more complex loading of the rachis during flight, which also includes torsion resulting from the longitudinal curvature of the rachis along its length.

A frame-by-frame analysis enabled the synchronization of the strain recordings with the wingbeat kinematics. Fig. 2B shows an expanded recording of the strain developed in the tenth wing beat as the bird passed the camera. Phases of the wing beat are labeled according to the terminology of Brown (1948). The upstroke begins with a phase termed the 'backwards flick' during which the bent wings are powerfully retracted. This phase of the wing stroke is characterized by a large tensile strain peak (0.0017), indicating a force directed anteriorly with respect to the bird (ventrally with respect to the feather). The orientation of the net force on the feather shaft appears to shift dorsally with respect to the feather during the 'extension' phase prior to the beginning of the downstroke. Brown (1948) distinguished between the early adduction phase of the downstroke, which he called the 'downstroke', and the later protraction phase, which he termed the 'forward swing'. Strain was compressive throughout the downstroke, reaching a peak magnitude of –0.0034 in the middle of the 'forward swing', at a point in time after which wing depression at the shoulder is nearly complete.

Histograms of peak compressive strains digitized from the recordings obtained from six feathers are displayed in Fig. 3. The mean peak strains recorded from individual feathers varied from as low as –0.0021 to as high as –0.0053, averaging –0.0033±0.0012 for the pooled sample (mean ± S.D., *N*=231 wing beats). Although these recordings were made from different feathers on different birds, the data suggest somewhat higher peak strain magnitudes in the distal feathers. This pattern is supported by an examination of peak strains recorded from different feathers within the same individual, for which higher strains were measured in the more distal feather of the two birds in which such a comparison could be made (pigeon 1, $P<0.0001$, *N*=26 wing beats; pigeon 6, $P<0.0001$, *N*=37; Mann–Whitney *U*-test). However, given the small sample of feathers for which we were able to obtain successful strain recordings, this result can only be considered suggestive until additional data become available.

Mechanical failure properties of feather shafts

The four-point bending tests demonstrated that flight feather shafts are much more likely to fail by local buckling than by rupture of the tensile surface. Of the 15 feather shafts loaded to failure, only one shaft actually failed by tensile fracture (which we suspect was probably due to structural damage incurred prior to testing). The mean bending moment at failure was 0.20±0.03 N m (mean ± S.D., *N*=15), corresponding to a compressive stress of 137±26 MPa. Cross-sectional data

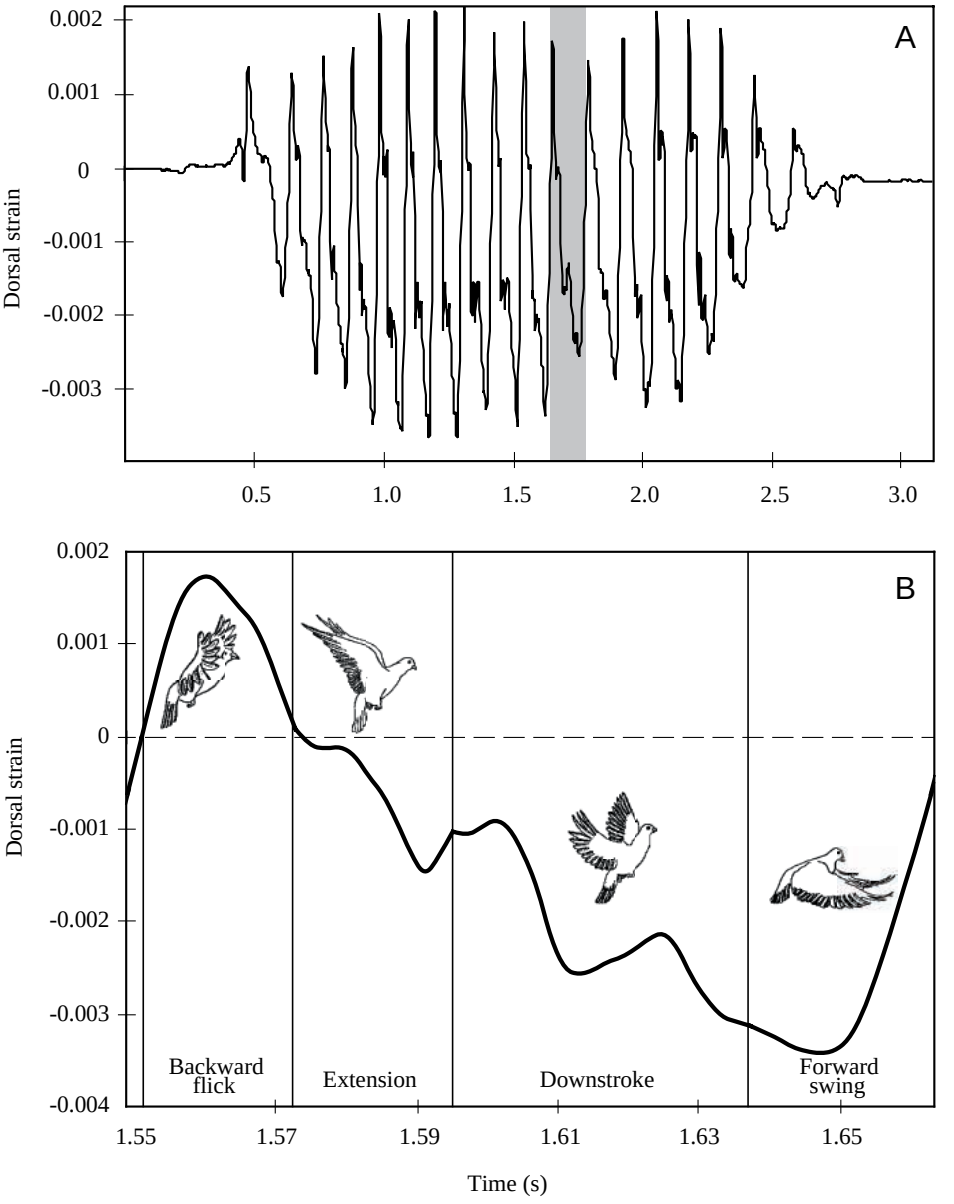

Fig. 2. (A) Representative strains recorded from the dorsal surface of a ninth primary feather shaft for an entire flight sequence. Lift forces produce negative (compressive) strains, so negative peaks occur during the downstroke and positive (tensile) peaks occur during the upstroke. The bird began the flight with an upstroke to initiate its first downstroke. Peak compressive strains increased during the first four downstrokes and then remained fairly constant until after the bird had passed the video camera (shaded region). (B) An expanded recording of the strain recorded for the cycle during which the pigeon passed the camera. The line drawings (adapted from Brown, 1948) show the position of the wings during each part of the wingbeat cycle.

obtained from the feathers near the site of failure were used to calculate a theoretical buckling moment according to equation 4. The predicted values for buckling failure stress obtained from this calculation averaged 166±27 MPa, only slightly more than our empirically derived values.

Scanning electron micrographs of sections obtained from failed pigeon primary flight feather shafts are shown in Fig. 4. Fig. 4A shows a short section of a feather shaft that experienced local buckling of its dorsal surface; the predominant mode of failure observed during the four-point bending tests. Numerous transverse, as well as a few longitudinal, microfractures are observed at the site of failure, none of which completely broke through the dorsal wall of the section (the longitudinal axis of the feather runs obliquely from upper left to lower right in the micrograph). This behavior appears to typify local buckling, which is a complex mode of failure entailing first a gradual flattening of the cross section and then a catastrophic collapse of the cross section due to components of stress perpendicular to the compressive surface of the structure (Brazier, 1927). In contrast, Fig. 4B shows the fractured surface of a section of the rachis loaded to failure in uniaxial tension, revealing that tensile failure occurs primarily along a plane parallel to the fibers and oblique to the surface of the cortex. Fig. 4C shows an oblique end-on view of the fractured ends of the same section at a higher magnification. Fig. 4B,C suggests that fracture of the shaft was initiated along planes of weakness between fibers, which continued to separate until the cross-sectional area of intact fibers had decreased to a critical size. At this point, the stress within the fibers would have built up to exceed the tensile breaking strength of the keratin, causing rapid rupture of the section.

Analysis of failure mode

Given a structure with consistent material properties, the

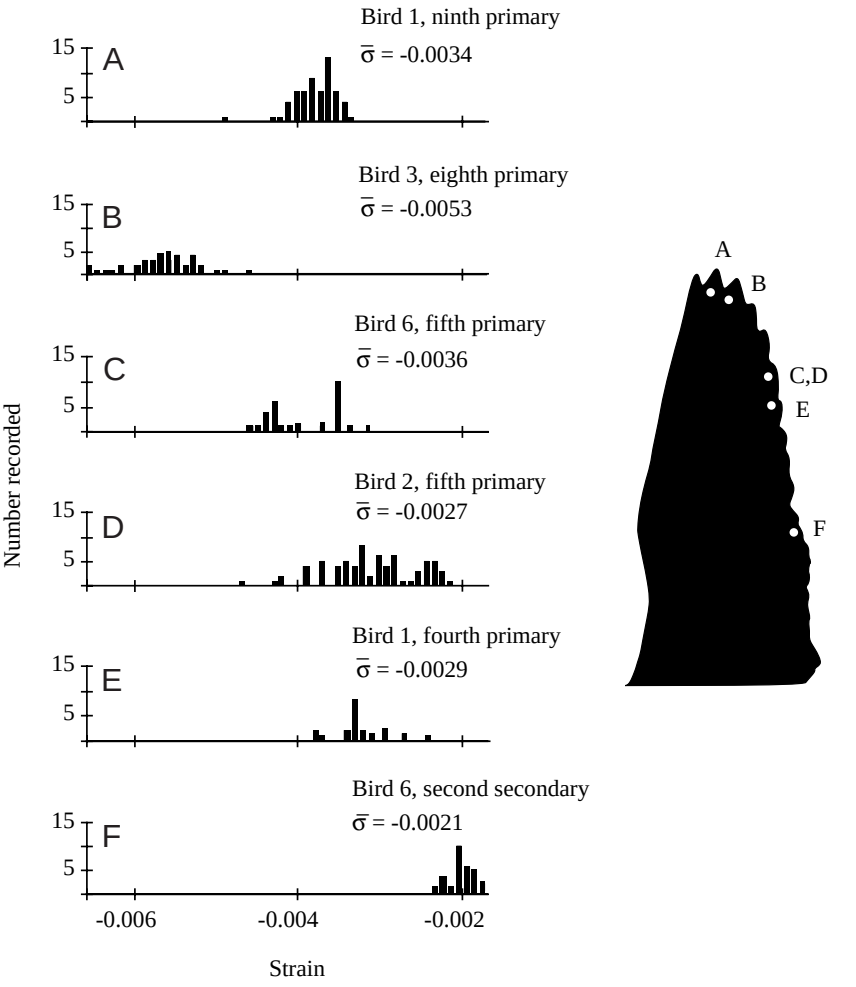

Fig. 3. Histograms showing the sampled frequency distributions of peak compressive strains recorded from six different flight feathers (A–F), ordered from distal to proximal location within the wing. The location of each of the feathers is shown on the silhouetted wing to the right. Mean peak strain $\bar{\sigma}$ is also shown for each feather.

mode of failure can sometimes be predicted on the basis of an analysis of cross-sectional shape (Currey and Alexander, 1985). Fig. 5 shows the theoretical critical bending moments that would cause failure in a feather shaft due to: (1) fracture of the tensile surface; (2) local buckling; and (3) surface wrinkling, calculated using equations 3, 4 and 5, respectively. For each failure mode, the critical bending moment decreases towards the feather tip because the shaft tapers distally. The lowest curve (cortex wrinkling) indicates the most likely failure mode because, as a feather is bent to failure and the bending moment increases from zero, it must first pass through a lower curve before reaching a value indicated by the next highest curve specified by another failure mode. Tensile fracture, therefore, is the least likely mode of failure along the entire length of the feather shaft. The critical bending moments predicted by the sandwich and the thin-walled cylinder models, however, are fairly similar and consistent over the length of the rachis. Nevertheless, their predicted critical failure moments are only approximately 50 % of the empirically derived values.

Safety factor during flight

Using a value of 2.5 GPa for the elastic modulus of feather keratin (Bonser and Purslow, 1995; Crenshaw, 1980), the mean (–0.0033) and maximum (–0.0063) peak compressive strains recorded from the flight feathers during slow level flight correspond to mean and maximum peak stresses of –8.3 and –15.7 MPa, respectively. These stress values indicate a safety factor ranging from 9 to 17 under these conditions on the basis of our empirically derived estimate of 137 MPa for the buckling strength of the feather shaft. Given the uncertainty of correcting for strain gauge reinforcement of the feather rachis, these estimates of safety factor should be treated with caution.

Discussion

In vivo *strain recordings*

In comparing our results for feather strains with other avian flight data, it is important to bear in mind that these data were obtained for slow flight. The wing kinematics were qualitatively similar to those described by Brown (1948) and Tobalske and Dial (1996) for the slow flight of pigeons, during which the wing tips moved in a characteristic ‘figure-of-eight’ pattern. This indicates that the birds were probably using a vortex ring gait (Rayner, 1995; Tobalske and Dial, 1996). The wing tips were invariably brought very close to one another during the reversal at the end of the downstroke, to the extent that one of the birds clearly crossed its wing tips at this time.

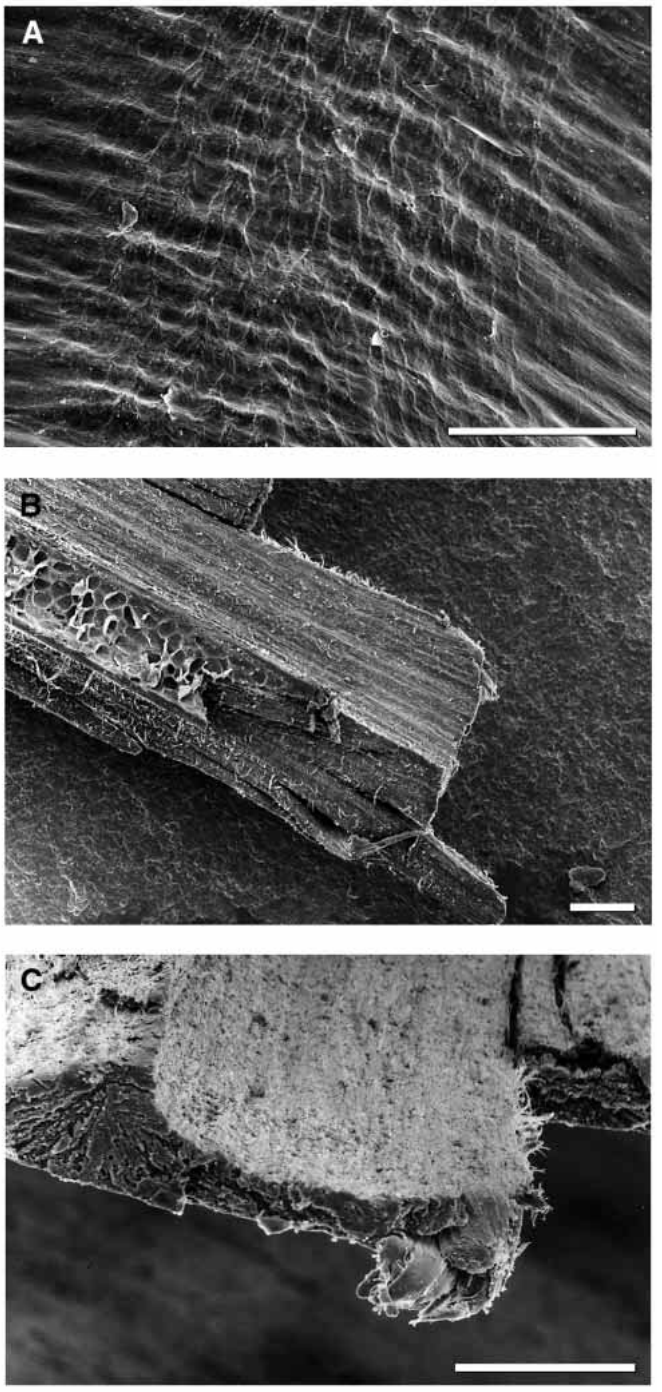

Fig. 4. Scanning electron micrographs of feather shafts loaded to failure. (A) Dorsal view of a region of the rachis that failed in buckling. The longitudinal axis of the rachis runs obliquely from upper left to lower right. Numerous microfractures are evident, most of which appear to run transversely to the shaft. (B) An interior view of the fracture surface of a feather shaft that was loaded in tension to failure. Some of the medullary foam that remained attached to the cortex is visible on its internal surface. The fracture appears to follow planes of weakness between keratin fiber bundles until the cross-sectional area of intact fibers was reduced to a critical size. At this point, the remaining intact fibers appear to have ruptured. (C) An oblique end-on view of the feather section displayed in B, showing a magnified view of the ruptured fibers. Scale bars, 100 μm.

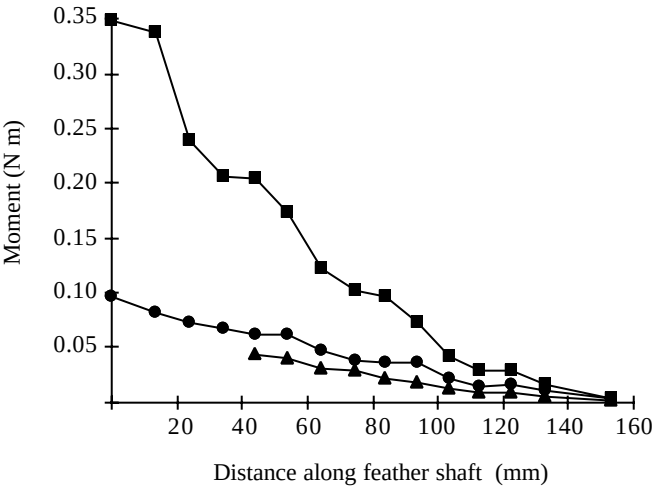

Fig. 5. A comparison of theoretical critical bending moments to cause failure along a feather shaft. Critical bending moments were calculated on the basis of the digitized shape for a series of 15 cross sections along the length of a feather, using the three failure models described in the text: (■) the critical bending moment for the feather shaft modeled as a beam that fails by tensile rupture (equation 3); (●) the critical bending moment that produces local buckling failure of the shaft when modeled as a thin-walled cylinder (equation 4); (▲) the critical bending moment of a composite foam sandwich that fails by wrinkling of the compressive surface (equation 5).

This pattern of wing tip reversal at the end of the downstroke may aid in the closing and shedding of a vortex ring before the initiation of the following upstroke (Rayner, 1995).

The time course of strain recorded from the flight feathers in this study differs from the pattern of pectoralis muscle force development during the downstroke (Fig. 6) on the basis of calibrated bone strains recorded directly above the insertion of the pectoralis muscle on the deltopectoral crest of the humerus (Biewener et al. 1998; Dial and Biewener, 1993). Whereas the compressive peak in feather strain occurs during the ‘forward swing’, pectoralis muscle force peaks much earlier during the first half of the downstroke. The peak in feather strain occurs at a point in the wingbeat cycle during which the wings are simultaneously supinated, adducted and protracted so that the ventral surfaces oppose each other in front of and below the bird’s body. Consequently, much of the force acting on the feathers at this time is oriented laterally and, therefore, cannot provide much thrust or weight support. Because the aerodynamic force acting on the feathers opposes the inertia of the wing, we speculate that the bird may rotate its wings during the forward swing in order to increase profile drag, thereby decreasing the amount of muscle force needed to decelerate the wing prior to the wing tip reversal.

Although peak strains measured at the dorsal surface of the rachis were always compressive, high-magnitude tensile strains were recorded in the primaries during the ‘backward flick,’ signifying a net force directed ventrally with respect to the feather or anteriorly with respect to the bird. It is possible that some of this strain is due to the inertia of the feather

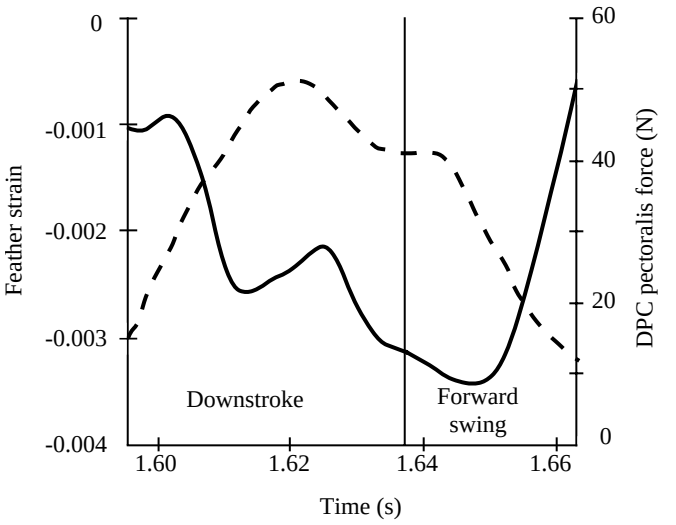

Fig. 6. A comparison of the timing of dorsal strain recorded from a ninth primary (solid line) relative to pectoralis muscle force development (dashed line; data from Biewener et al. 1998) during the downstroke and forward swing (see Fig. 2B). Feather strain on the dorsal surface of the rachis is compressive during the downstroke, reaching its greatest magnitude during the 'forward swing'. In contrast, peak pectoralis force develops much earlier during the downstroke. Force measurements of the pectoralis are based on calibrated measurements of strain developed within the deltopectoral crest (DPC) of the humerus.

causing it to bend forward in response to the backward acceleration of the wing. Nevertheless, the magnitude of peak tensile strain seems to be large enough in comparison with the peak compressive strains measured during the downstroke to suggest the possibility of useful force generation. Aldridge (1987) and Brown (1951) considered the possibility that profile drag on the dorsal wing surface could produce thrust during this early phase of the upstroke. However, Rayner (1991) contended that flow visualization observations do not provide evidence of aerodynamic force production during this phase of the upstroke. Our results suggest that this issue deserves further attention.

Safety factor of the rachis

While the concept of a safety factor is both simple and elegant, many complications can arise when applying it to animal structures. For example, it is often difficult to ascertain whether the data are representative of maximal performance. Clearly, in our present study, this was not the case. In a previous study of pigeons flying near their performance limit (carrying their full body weight on their backs), humeral bone strains were found to be approximately 40 % higher than those during slow flight (Biewener and Dial, 1995). Consequently, we might expect a comparable 1.4-fold increase in feather shaft stresses under these more strenuous flight conditions. Such an increase would lower the safety factor of the feathers to between 6 and 12. This is compounded by the uncertainty of our estimates used to correct for gauge reinforcement of the feather rachis. Because feather shafts are curved (concave posteriorly), distally applied forces not only bend but also pronate (twist) the feather shaft. This will subject the shaft to significant torsion, which is known to lower the critical bending moment needed to cause local buckling failure in thin-walled cylinders (Young, 1989). As a result, feather shafts can be expected to buckle at lower bending moments *in vivo* than those measured in four-point bending. Owing to the practical difficulties associated with attaching rosette strain gauges, or even attaching single-element strain gauges along the estimated shear strain axis of the feathers of a live bird, we were unable to measure torsion during flight. On the basis of measurements of the longitudinal curvature of the rachis, we estimate that the torsional moment is probably less than 20 % of the bending moment. This suggests that our results overestimate the safety factor of the rachis, but not by a substantial amount.

How do our safety factor estimates for feather shafts compare with safety factors measured in the wing skeleton? On the basis of their relatively high cost of use and the low cost of failure, we predicted that the safety factor of flight feather shafts would be less than or equal to the safety factor for the wing bones. However, safety factors for avian wing bones appear to be much lower. Biewener and Dial (1995) reported a safety factor of 3.5 for the humerus of a pigeon loaded in bending, and 1.9 for the same bone loaded in torsion on the basis of *in vivo* shear strain recordings. Kirkpatrick (1994) calculated a mean safety factor of 2.2 for wing bones from 14 different species on the basis of quasi-steady aerodynamic models and loading tests of bending strength. In another study, Swartz *et al.* (1992) obtained a similar safety factor (3.9) for both bending and shear strains in the wing bones of megachiropteran bats during flight.

At least three factors could contribute to why the safety factor of feathers is much higher than for the wing bones. First, the lack of a mechanism for repairing any damage that accumulates over long periods of use can be expected to favor an increased safety factor. In the present study, however, this is unlikely to be an important consideration since our mechanical tests of breaking strength were carried out on molted feathers, which had presumably accumulated a year's worth of damage. Second, it may be that feathers must resist stresses greater than those induced by aerodynamic forces during flight. Accidental collisions with branches or other hard objects could cause high local stresses in the feather shaft. Observations of feather damage in our caged birds indicate, however, that damage typically affects the feather vanes before the shaft, leading us to discount this as a significant factor. A third, and we believe more likely, explanation is that feathers are constrained more by their need to be stiff than their need to be strong.

Feathers must be sufficiently stiff to transmit aerodynamic forces effectively to the musculoskeletal system and to resist excessive shape change during flight. Their flexural stiffness (EI) depends both on the cross-sectional shape of the rachis and the Young's modulus of the feather keratin (Wainwright

et al. 1976). A comparison of the material properties of feather keratin with those of vertebrate bone helps to explain why flight feather shafts appear to be built with a greater surplus of strength than the wing bone elements. Although the tensile breaking strengths of avian bone (180 MPa; McAlister and Moyle, 1983) and feather keratin (226 MPa; Crenshaw, 1980) are comparable, the Young's modulus of bone (13 GPa; McAlister and Moyle, 1983) greatly exceeds that of keratin (2.5 GPa; Bonser and Purslow, 1995; Crenshaw, 1980). Therefore, even though similarly shaped (equal second moments of area) structures built of bone and keratin would have similar strengths, the bone element would be five times more stiff. Consequently, for the keratin element to have an equal flexural stiffness, its structural form would require a second moment of area five times greater than that of the bone. This increase in second moment of area, however, would also augment the failure strength and safety factor of the keratin structure with respect to that of the bone. Consistent with this, the relative wall thickness to radius ratio (t/R) of pigeon feather shafts (0.081±0.038, mean ± S.D., N=24) near the base of the rachis in the same region as the strain recordings) is less than 50 % of that of wing bones (range 0.17–0.31; Currey and Alexander, 1985; W. R. Corning, unpublished observations).

The high safety factor of feather shafts (which again depends on our ability to estimate reliably the effect of strain gauge reinforcement) is therefore likely to reflect the need for achieving a high stiffness while, at the same time, being lightweight. As feathers are epidermal structures that probably evolved from specialized reptilian scales (Maderson, 1972), their structural design also reflects a phylogenetic constraint of the material from which they are constructed. As birds evolved flight feathers, the flexural stiffness of the shafts was probably limited by the compliance of keratin, of which the ancestral reptilian scales were composed. Interestingly, the observation that the Young's modulus of feather keratin is higher and yields at a much higher stress than that of snake skin epidermis (Fraser and Macrae, 1980) suggests the possibility that the material properties of feather keratin may have evolved since the divergence of the lepidosaurian and avian lineages to enhance flight performance. Nevertheless, changes in the cross-sectional shape of the rachis were most important in achieving a stiff yet lightweight design favorable to the function of the wing as an airfoil for flight.

The authors would like to thank The University of Chicago biomechanics discussion group and Drs R. McNeill Alexander, David Konieczynski, Raphael Lee and Michael LaBarbera for helpful comments at various stages of the work. We also appreciate the help of Mr John Gilpin, who machined components of the tensometer and four-point loading jig. The Field Museum of Natural History and Ms Betty Strack deserve special thanks for producing the electron micrographs. This work was supported by NSF grants IBN-9306793 and IBN-9723699 to A.A.B. and an NSF multi-user instrumentation grant BIR-9318129.

References

ALDRIDGE, H. D. J. N. (1987). Body accelerations during the wing beat in six bat species – the function of the upstroke in thrust generation. *J. exp. Biol.* **130**, 275–293.

ALEXANDER, R. MCN. (1981). Factors of safety in the structure of animals. *Scient. Prog. Oxford* **67**, 109–130.

BIEWENER, A. A. (1993). Safety factors in bone strength. *Calcif. Tissue Int.* **53**, S68–S74.

BIEWENER, A. A., CORNING, W. R. AND TOBALSK, B. W. (1998). *In vivo* pectoralis muscle force–length behavior during level flight in pigeons (*Columba livia*). *J. exp. Biol.* (in press).

BIEWENER, A. A. AND DIAL, K. P. (1995). *In vivo* strain in the humerus of pigeons (*Columba livia*) during flight. *J. Morph.* **225**, 61–75.

BONSER, R. H. C. (1996). The mechanical properties of feather keratin. *J. Zool., Lond.* **239**, 477–484.

BONSER, R. H. C. AND PURSLOW, P. P. (1995). The Young's modulus of feather keratin. *J. exp. Biol.* **198**, 1029–1033.

BRAZIER, L. G. (1927). On the flexure of thin cylindrical shells and other 'thin' sections. *Proc. R. Soc. Lond. A* **116**, 104–114.

BROWN, R. H. J. (1948). The flight of birds: flapping cycle of the pigeon. *J. exp. Biol.* **25**, 322–333.

BROWN, R. H. J. (1951). Flapping flight. *Ibis* **93**, 333–359.

CRENSHAW, D. G. (1980). Design and materials of feather shafts: very light, rigid structures. *Symp. Soc. exp. Biol.* **43**, 485–486.

CURREY, J. D. AND ALEXANDER, R. MCN. (1985). The thickness of the walls of tubular bones. *J. Zool., Lond.* **206**, 453–468.

DIAL, K. P. AND BIEWENER, A. A. (1993). Pectoralis muscle force and power output during different modes of flight in pigeons. *J. exp. Biol.* **176**, 31–54.

FRASER, R. D. B. AND MACRAE, T. P. (1980). Molecular structure and mechanical properties of keratins. *Symp. Soc. exp. Biol.* **34**, 211–246.

GIBSON, L. J. AND ASHBY, M. F. (1988). *Cellular Solids: Structures and Properties.* New York: Pergamon.

GILL, F. B. (1995). *Ornithology*. New York: W. H. Freeman & Company.

HAHN, K. AND LABARBERA, M. (1993). Failure of limb segments in the blue crab, *Callinectes sapidus* (Crustacea, Malacostraca). *Comp. Biochem. Physiol.* **105**A, 735–739.

HERTEL, H. (1966). *Structure, Form, Movement.* New York: Reinhold Publishing Corp.

KIRKPATRICK, S. J. (1994). Scale effects on the stresses and safety factors in the wing bones of birds and bats. *J. exp. Biol.* **190**, 195–215.

LOWELL, R. B. (1985). Selection for increased safety factors of biological structures as environmental unpredictability increases. *Science* **228**, 1009–1011.

MADERSON, P. F. A. (1972). On how an archosaurian scale might have given rise to an avian feather. *Am. Nat.* **106**, 424–428.

MCALISTER, G. B. AND MOYLE, D. D. (1983). Some mechanical properties of goose femoral cortical bone. *J. Biomech.* **16**, 577–589.

NIKLAS, K. J. (1989). Safety factors in vertical stems – evidence from *Equisetum hyemale*. *Evolution* **43**, 1625–1636.

PURSLOW, P. P. AND VINCENT, J. F. V. (1978). Mechanical properties of primary feathers from the pigeon. *J. exp. Biol.* **72**, 251–260.

RAYNER, J. M. V. (1991). Wake structure and force generation in avian flapping flight. *Acta XX Congr. int. Orn.* **2**, 702–715.

RAYNER, J. M. V. (1995). Dynamics of the vortex wakes of flying and swimming vertebrates. *Symp. Soc. exp. Biol.* **49**, 131–155.

RUTSCHKE, E. (1976). Gross structure in bird feathers. In *Proceedings of the XVIth International Ornithological Congress*, vol. 16, pp. 414–425. Canberra, Australia: Australian Academy of Science.

SWARTZ, S. M., BENNETT, M. B. AND CARRIER, D. R. (1992). Wing bone stress in free flying bats and the evolution of skeletal design for flight. *Nature* **359**, 726–729.

TOBALSKE, B. W. AND DIAL, K. P. (1996). Flight kinematics of black-billed magpies and pigeons over a wide range of speeds. *J. exp. Biol.* **199**, 263–280.

WAINWRIGHT, S. A., BIGGS, W. D., CURREY, J. D. AND GOSLINE, J. M. (1976). *Mechanical Design in Organisms.* Princeton: Princeton University Press.

WORCESTER, S. E. (1996). The scaling of the size and stiffness of primary flight feathers. *J. Zool., Lond.* **239**, 609–624.

YOUNG, W. C. (1989). *Roark's Formulas for Stress and Strain.* New York: McGraw-Hill.